Classification : PHYSICAL SCIENCES : Applied Physical Sciences

Magnetoelectrochemical control of a chemical spin valve

Petru Lunca [*], Neil T. [*], Hicham , Guillaume ,

Vina , Christian [,d], Riccardo and Bernard

[a] Centre de Recherche Public Gabriel Lippmann, Département SAM!, 41, rue du Brill!, L - 4422 Belvaux, Luxembourg

[b] Department of Physics, University of Hull, Cottingham Road, Kingston-upon-Hull, HU6 7RX, United Kingdom

[c] Institut de Physique et Chimie des Matériaux de Strasbourg (IPCMS) and Laboratory NIE, University of Strasbourg, UMR 7504 CNRS-UdS, 23 rue du Loess, 67034 Strasbourg, France

[d] Peter Grünberg Institut (PGI-6), Forschungszentrum Jülich GmbH, D-52428 Jülich, Germany

* these authors contributed equally to this work

Corresponding author: B. Doudin, Institut de Physique et Chimie des Matériaux de Strasbourg (IPCMS), UMR 7504 CNRS-UdS, 23 rue du Loess, 67034 Strasbourg, France

Tel : + 33(0)388 107249

Email : bdoudin@unistra.fr

Keywords: spintronics, magnetohydrodynamics, supramolecular chemistry

Abstract. In the field of spintronics, the archetype solid-state two-terminal device is the spin valve, where the resistance is controlled by the magnetization. We show here how this concept of spin-dependent switch can be extended to magnetic electrodes in solution, by magnetic control of their chemical environment. Appropriate nanoscale design allows a huge enhancement of the magnetic force field experienced by paramagnetic molecular species in solutions, which changes between repulsive and attractive on changing the electrodes' magnetic orientations. Specifically, the field gradient force created within a sub-100 nm sized nanogap separating two magnetic electrodes can be reversed by changing the orientation of the electrodes magnetization relative to the current flowing between the electrodes. This can result in a breaking or making of an electric nanocontact, with a change of resistance by a factor of up to . The results reveal how an external field can impact chemical equilibrium in the vicinity of nanoscale magnetic circuits.

Significance Statement. The magnetic gradient force field offers numerous possibilities to position and manipulate magnetic nanoparticles, but has limited influence on paramagnetic molecules in solutions. We show here how proper design and miniaturization of ferromagnetic electrodes create huge force fields, manipulated by an externally applied field. Its influence on chemical reactions is revealed by an example on a Ni metallic nanobridge, of conduction drastically modified when the Ni redox reactions equilibrium is shifted under magnetic control. This is the chemical version of the solid-state spin valve device. While the importance of the magnetic field amplitude on chemical reactions is well documented, our findings suggest that the magnetic field gradient can become a dominant influencing factor on chemical reactions at the nanoscale.

\body

Spintronics (1, 2) is a mature research field in solid-state physics, with important electronic device applications. Spin-dependent transport studies in a liquid environment are much scarcer, and still rely on solid-state spintronics devices concepts. For example, giant magnetoresistance or tunnel magnetoresistance spin valves (3) are used for detecting the stray magnetic field (4) of nearby µm-sized (bio-active) magnetic beads (5). The objects studied are significantly larger than the molecular scale, owing to the predominant concentration gradient and Brownian forces exceeding by orders of magnitudes the magnetic force experienced by paramagnetic molecules (6). However, miniaturization of ferromagnetic elements below the micrometer range provides opportunities for enhancing the magnetic force field, making the detection of single spin possible (7). We propose here to use such a nanoscale enhancement strategy to investigate how the realization of very large magnetic field gradients can impact the properties of paramagnetic molecules, in particular by modifying their chemical equilibrium. An external magnetic field controls the magnetization direction of ferromagnetic immersed electrodes, with a related large change of the magnetic forces in their vicinity. This modifies accordingly the chemical stability of the solution, in the interesting case where paramagnetic molecules are essential to the construction of a conductive molecular-sized system. The resulting metallic nanobridge therefore exhibits electrical properties tunable through a change of magnetic orientations of the electrodes. While it relies on a totally different physical origin, this is the chemical analog of a solid-state spin valve device.

We illustrate this concept by presenting magnetoresistance (MR) results for a Ni-based nanobrige separating two nearby Ni electrodes immersed in an electrochemical solution. The experiments are based upon reduction (oxidation) of Ni^{++} ions (Ni metal) on these electrodes used as working electrodes kept under potentiostatic conditions in an electrochemical cell, with MR investigations performed after an electrodeposited metallic Ni bridge is stabilized between the two nearby electrodes. Lab-on-chip microfluidic circuitry directs the electrolyte flow (Fig. 1), with an external valve system allowing change of the chemical environment. Since measurements are performed *in-situ* in an electrolyte, we take advantage of microfluidic control of the composition of the bath to reveal unambiguously how a change in the chemical bath impacts the MR properties.

The two facing planar electrodes are first patterned with a typical separation in the 50 -100 nm range. They serve as working electrodes (, , Fig. 1) and share the same imposed potentiostatic conditions for reducing metal ions in solutions. Electrodeposition of a metallic film of thickness in the range of the separation between electrodes results in the fabrication of a metallic nanobridge (Fig. 1). Full data and details for fabricating Ni, Co, or Ag metallic nanobridges down the few atoms size are presented in our previous work (8, 9, 10, 11) and more details are given in the Supplementary Information. More specifically, diminution of the initial gap between the two nearby patterned working electrodes occurs by reduction of Ni^{++} ions under constant negative potential , referred to a Pt or Ag/Cl electrode (*R*, Fig. 1). It results in electroplating a Ni film of 20-50 nm thickness over the whole surface of the two electrodes , . A small superimposed monitoring AC excitation between and provides a diagnostic of the impedance separating and and reveals the making or breaking of the Ni bridge by recording the impedance between the electrodes. A clear transition from a capacitive behavior to purely

resistive contact occurs below several kΩ impedance value. The plotted AC conductance in Fig. 1 corresponds to the real part of the impedance diagnostic measurement, and is not indicative of the DC electrolytic current in the cell. If a less negative voltage is applied, the contact can re-open when oxidation of the metallic Ni bridge prevails, occurring at . Control and stabilization of the contact impedance is obtained by an iterative step approximation. The typical procedure is to close a contact, and then reach a potentiostatic condition to a value , using 10 mV steps increments, until the conductance of the nm-size Ni bridge remains stable over a typical time scale, with the sample impedance in the range 10 – 1000 Ω. The MR properties are then measured under external magnetic field sweep or magnetic field rotation, furthermore monitored while exchanging the high concentration Ni electrolyte with a solution containing the boric acid buffer only, keeping the bath pH around 4. Data are shown in conductance values in units of the quantum of conductance = /h ≈ 1/13 kΩ, following the literature of quantum ballistic transport studies in metallic nanocontacts (12).

Changing the direction of the saturating applied magnetic field has a dramatic influence on the conductance of Ni nanocontacts (Fig. 1). For sufficiently large field values (0.8 T in our case), the electrodes are magnetized in a well-defined saturated state along the applied field. Changing the field direction results in switching between the *OFF* conduction state of the sample when the field is longitudinal to the current direction (zero angle), and the *ON* state when transverse. The *ON/OFF* conductance ratio reaches , limited by the *OFF* leakage current resulting from the finite impedance between working and reference electrodes (measured in a typical Ω range by impedance spectroscopy at frequencies below 1kHz).

Fig. 2 details how this large AMR relies on the presence of Ni ions in solution. Microfluidic control allows a reversible change of the Ni ions concentration, keeping the

monitoring of the AMR properties. The region I of Fig. 2 corresponds to the data shown in Fig. 1b, with a reconstruction of the AMR curve from the time-dependent angle of the applied field synchronized with the time-dependent sample conductance values (Fig. 2b). The large oscillations disappear when the closed *ON* state is realized with the buffer electrolyte only present in the solution (Fig. 2, region II). For bulk metallic Ni, the anisotropic magnetoresistance (AMR) does not exceed a few percent, and follows a simple shape, signature of the influence of spin-orbit interactions on diffusive electric transport (13). This is indeed observed in the AMR reconstruction curve of the region II (Fig.2c), confirming that the sample is made of a metallic Ni contact, and that magnetostriction artifacts do not affect the observed properties (14). A remarkable recovery of the large AMR properties is found when re-inserting the Ni ions in the solution (Fig. 2, region III).

Another set of experiments was performed under variable magnitude magnetic field, which is the typical magnetoresistance measurement method for spin valve devices (Fig. 3): the MR curves in the regions 1, 2 of Fig. 3a reflect the AMR properties under the assumption that the low-field magnetic configuration does not correpond any more to the well-aligned saturation state. For the case of Fig 3, a low conductance is expected in the longitudinal magnetization state pinned at high fields. Partial magnetization rotation occurs at lower fields, with the transverse orientation increasing significantly the conductance, as previously indicated in the data of Fig. 2 (15). The data of Fig. 3 b,c also confirms the impressive long-term device stability: the memory of the MR properties of the first stage of the experiment (region 1 of Fig 3a) is nearly perfectly recovered in region 2 even though the contact spent 600s open (*OFF* state) when Ni ions were eliminated from the bath. A closer inspection of the evolution of the AMR after exchanging the solution reveals that the disappearance (re-appearance) of the large AMR is continuous in

amplitude (Fig. S1 in the SI) when decreasing (increasing) the Ni ions concentrations. Our data clearly indicates that a model of conduction in a solid-state device is not appropriate here. It shows unambiguously that Ni ions in the solution are at the origin of the remarkable AMR (MR)

A model detailing the influence of a magnetic field on paramagnetic ions can explain our findings. The paramagnetic Ni ions, of concentration C (in mol m^{-3}) in a solution, with molar magnetic susceptibility χ_m, (in mol^{-1}), are attracted to regions of high magnetic induction B (in tesla) with forces of density (in N m^{-3}):

$$\vec{f}_\nabla = \frac{C\chi_m}{2\mu_0}\vec{\nabla}(B^2)$$

where $\mu_0 = 4\pi \ 10^{-7}$ Hm^{-1} (16). This 'magnetic field gradient force' is proportional to the product of the scale-invariant field B with its gradient ∇B. The latter increases when decreasing the size of the system, and is therefore exacerbated at the nanoscale. This force prevails over forces related to the magnitude of B, and not its gradient. Magnetohydrodynamics usually refer to the Lorentz force, with the magnetic field modifying the trajectories of the electric current lines, and creating convection possibly modifying electrochemical equilibrium (17) or imposing chirality (18) when significant current densities are involved. In our case, with plating current densities not exceeding 5 μA/, the Lorentz force density remains below 100 N/ (for our magnetic field in the 1 T range), shown below to be several orders of magnitude smaller than the gradient force near our nanostructures.

Quantitative insight of the predominant magnetic gradient force in our device geometry is obtained using a micromagnetic code, which accounts for the structure of the magnetization and the resulting magnetostatic field (Ref. 19, 20, see details in SI). We limit ourselves to the saturated state, expected for Ni when applied fields exceed 0.5 T, and corresponding to our AMR

experimental conditions. This avoids ambiguity in the conclusions, as our modeling does not require any hypothesis for the magnetic configuration at low fields, where the relaxed state can be highly dependent on nanoscale minute defects in the real material geometry (Fig 1a). We find that our planar electrodes design creates a gradient field exceeding T/m. Such huge field gradients rival the highest values reported in the literature on single spin detection using scanning probe techniques (**Error! Bookmark not defined.**, 21), where searching for the highest magnetic gradient is a prerequisite for measurements sensitivity. The force field directions and amplitudes in our calculations are illustrated in Fig. 3, using a dimensionless susceptibility $C\chi_m = 7.5 \times 10^{-5}$ for a 1.8 M Ni^{++} paramagnetic ions concentration taking into account the diamagnetic property of water (see details in ref. **Error! Bookmark not defined.**). When the electrodes are magnetized along their length, or in a longitudinal direction with respect to the current direction, the force field of approximately radial symmetry reaches a magnitude of Nm^{-3}. It exceeds by three orders of magnitude the largest value we found in the literature (22). The transverse magnetization case produces a local inversion of the force field, being now repulsive for ions residing at the edge of the nanogap, with magnitudes similar to the longitudinal case (Fig. 4, with more details in Fig. S2 and Table S1 of the SI).

While magnetic forces are commonly used for positioning micro or nano-size magnetic particles, they cannot stabilize molecules: A single paramagnetic molecule, with a spin S (not exceeding a small multiple of 1/2), cannot gain more than $\frac{1}{2}g^2\mu_B^2 S(S+1)B^2/3kT$ energy when attracted by a field B. This is in the range of the Zeeman splitting energy, not exceeding the mK energy range in fields of the 1T range. Magnetic fields can possibly modify chemical reactions rates and yields when they proceed via spin correlated radical pair intermediates. These spin chemistry effects (23) can occur in a wide range of applied fields, depending on the

thermodynamic or quantum mechanical mechanism involved. The smallness of the Zeeman splitting magnetic energy can require rather large magnetic fields (of the order of 10 T magnitude) to impact the reaction (24). The hyperfine field, typically of the order of 0.1 T, can also significantly modify the lifetime of radical species, in the so-called 'normal magnetic field effect', extensively studied for photosynthesis. Lower-field effects, down to sub-mT field range, are of increasing importance, owing to the societal concerns on their effect on health (25). Note that these effects are unlikely to apply to our case, where the nanogaps always experience a significant field of 0.4 - 1 T for AMR studies, whatever the orientation of the external magnetic field is. Furthermore, correlated radical pairs typically result from a photo-excitation process, not applying in our case.

The thermal energy scale of 300K also relates to Brownian motion, which controls diffusive forces, of the order of $RT\nabla C$ per unit volume in a gradient of concentration ∇C. There is general agreement in the literature (**Error! Bookmark not defined.**, **Error! Bookmark not defined.**, 26, 27) that the diffusive forces dominate magnetic forces by orders of magnitude. Our scaling reasoning, explaining the numerical enhancement of the magnetic force field for our case, also applies to the diffusive forces. Magnetic gradient forces can nevertheless modify the convective flow around the electrodes in the presence of a transverse concentration gradient of electroactive species, possibly increasing the concentrations gradient and therefore enhancing diffusion (27, 28). Indeed, electrochemical studies showed that magnetic gradient (29) or Lorentz (ref. 30, negligible in our case) forces near working electrodes can possibly change the residency time of paramagnetic species at the electrodes and shifts the kinetics and equilibrium of the reactions (see for example refs. **Error! Bookmark not defined.**, 28, and references therein).

In our case, with force fields larger by orders of magnitude, the magnetic gradient force must impact even more the chemical equilibria of the redox reactions (Fig. 4). The observed hysteresis in the AMR curves of Fig. 2 can be explained by the irreversibility of the redox chemical reactions involving the Ni^{++} ions. The observed open/closed switch of conductance under applied field can be mapped to the potentiostatic conditions , , where open and closed nanocontacts are favored. Experimentally, the difference between these two potential values is around 100 mV. The non-reversibility of the redox reactions makes this difference history dependent, typically decreasing under successive open-close potential sequences, from an initial value as large as 300 mV down to values always exceeding 50 mV. This provides a straightforward rough estimate of the contribution of the magnetic field to the free energy of the system, i.e. on the order of 10 kJ/mol ($\approx$100 meV/molecule), tunable through magnetic control of the electrodes. This value is large enough to overcome an energy activation barrier, modify significantly the reaction rates, or provide opportunities to (de)stabilize weak chemical bonds. For example, we recently found that a magnetic (sub)layer was necessary to self-assemble highly conductive supramolecular architectures between electrodes with nanoscale separation (31). As this particular self-assembly is controlled by the presence of paramagnetic radicals, their attraction to magnetic electrodes might drive the delicate chemical equilibrium towards self-construction. More generally, the stability of supramolecular architectures, where energetic contributions to the total free energy of the order of can significantly impact the molecular configurations, can therefore become sensitive to the magnetic forces at the vicinity of magnetic nanostructures. This opens new possibilities for acting on chemical processes relevant to life sciences, where supramolecular interactions prevail (32).

The field of magnetophoresis, currently implicitly related to magnetic manipulation of nanoparticles, is hereby extended to magnetic forces on paramagnetic molecules in solution, where extreme force field conditions at the vicinity of magnetic nanostructures can be generated without the need of a very large external magnetic field source. We have shown here that this phenomenon can be used for creating new types of spin-sensitive devices. We also propose a new tabletop tool and methodology for influencing chemical reactions. Our findings suggest that the reaction yields or the chemical equilibrium, known to be sensitive to the magnetic field magnitude when intermediate radical species are involved, can also be influenced by the gradient of the magnetic field.

References

1. Zuti¢ I, Fabian J, Das Sarma S (2004) Spintronics: Fundamentals and applications. Rev. Mod. Phys. 76: 323-410.
2. Wolf SA, et al. (2001) Spintronics: A spin-based electronics vision for the future. Science 16: 1488-1495.
3. Johnson M (2004) Magnetoelectronics, Elsevier B.V., Amsterdam.
4. Graham DL, Ferreira HA, Freitas PP (2004) Magnetoresistive-based biosensors and biochips. Trends in Biotechnology 22: 455-462.

5.   Dobson J (2008) Remote control of cellular behaviour with magnetic nanoparticles. Nature Nanotech. 3: 138-143.

6.   Coey JMD, Aogaki R, Byrne F, Stamenov P. (2009) Magnetic stabilization and vorticity in submillimeter paramagnetic liquid tubes. Proc. Natl. Acad. Sci. USA 106(22): 8811-8817.

7.   Rugar D, Budakian R, Mamin HJ, Chui BW (2004) Single spin detection by magnetic resonance force microscopy. Nature 430: 329-331.

8.   Yang CS, Zhang C, Redepenning J, Doudin B (2004) In-situ magnetoresistance of Ni nanocontact. Appl. Phys. Lett. 84: 2865-2867.

9.   Lunca Popa P, et al. (2011) Hetero-nanojuctions with atomic size control using a lab-on-chip electrochemical approach with integrated microfluidics. Nanotechnology 22: 215302 1-7.

10.   Yang CS, Zhang C, Redepenning J, Doudin B (2004) Anisotropy magnetoresistance of quantum ballistic nickel nanocontacts, J. Mag. Mag. Mater. 286: 186-190.

11.   Sokolov A, Zhang C, Tsymbal E, Redepenning J, Doudin B (2007) Quantized Magnetoresistance in Atomic-Size Contacts. Nature Nanotech 2: 171-175.

12.   Agrait N, Yeyati AL, van Ruitenbeek JM (2003) Quantum properties of atomic-sized conductors. Physics Reports 377: 81-279.

13.   McGuire TR, Potter RI (1975) Anisotropic magnetoresistance in ferromagnetic 3d alloys. IEEE Trans. Magn. 11: 1018-1038.

14.   Müller M, et al. (2011) Conductance tuning of Dy break junctions by magnetostriction. Nano Letters 11: 574-578.

15.   Doudin B, Viret M (2008) Ballistic magnetoresistance? J. Phys.: Condens. Matter 20: 083201

16.   Rosensweig A (1997) Ferrohydrodynamics, Dover, New York.

17.   Monzon LMA, Coey JMD (2014), Magnetic fields in electrochemistry: The Lorentz force. A mini-review. Electrochem. Commun, in press.

18.   Mogi I, Morimoto R, Aogaki R, Watanabe K (2013) Surface chirality induced by rotational electrodeposition in magnetic fields. Sci. Rep. 3: 2574.

19.   Fredkin DR, Koehler TR (1990) Hybrid method for computing demagnetizing fields. IEEE Trans. Magn. 26: 415-417.

20.   Gliga S, Hertel R, Schneider CM (2008) Switching a magnetic antivortex core with ultrashort field pulses. J. Appl. Phys. 103: 07B115.

21.   Mamin HJ, Rettner CT, Sherwood MH, Gao L, Rugar D (2012) High field-gradient dysprosium tips for magnetic resonance force microscopy, Appl. Phys. Lett. 100: 013102.

22.   Chaure NB, Coey JMD (2009) Enhanced Oxygen Reduction at Composite Electrodes Producing a Large Magnetic Gradient. J. of The Electrochem. Soc. 156: F39-F46.

23.   Steiner UE, Ulrich T (1989) Magnetic field effects in chemical kinetics and related phenomena. Chem. Rev. 89: 51-147

24.   Steiner UE, Gilch P. (2003) High magnetic fields in chemistry, in : High magnetic fields, Theory and Expertiments I, ed. Fritz Herlach, Singapore, World Scientific.

25.   Timmel CR, Henbest KB (2004) A study of spin chemistry in weak magnetic fields. Phil. Trans. R. Soc. Lond. A 362: 2573-2589.

26.   Dunne P, Mazza L, Coey JMD (2011) Magnetic structuring of electrodeposits. Phys. Rev. Lett. 107 : 024501.

27. Dunne P, Coey JMD (2012) Patterning metallic electrodeposits with magnetic arrays. Phys. Rev. B 85 :224411.
28. Uhlemann M, et al. (2013) Structured electrodeposition in magnetic gradient fields. Eur. Phys. J. Special Topics 220: 287-302
29. Dass A, Counsil JA, Gao X, Leventis N (2005) Magnetic Field Effects on the Open Circuit Potential of Ferromagnetic Electrodes in Corroding Solutions. J. Phys. Chem B 19: 11065-11073.
30. Rhen FMF, Coey JMD (2007) Magnetic Field Induced Modulation of Anodic Area: Rest Potential Analysis of Zn and Fe. J. Phys. Chem. C 111: 3412-3416.
31. Faramarzi V, et al. (2012) Light triggered self-construction of supramolecular organic nanowires as metallic interconnects. Nature Chem. 4: 485- 490.
32. Lehn JM (1985) Supramolecular Chemistry: Receptors, Catalysts, and Carriers. Science 227: 849–856.

Figure Legends
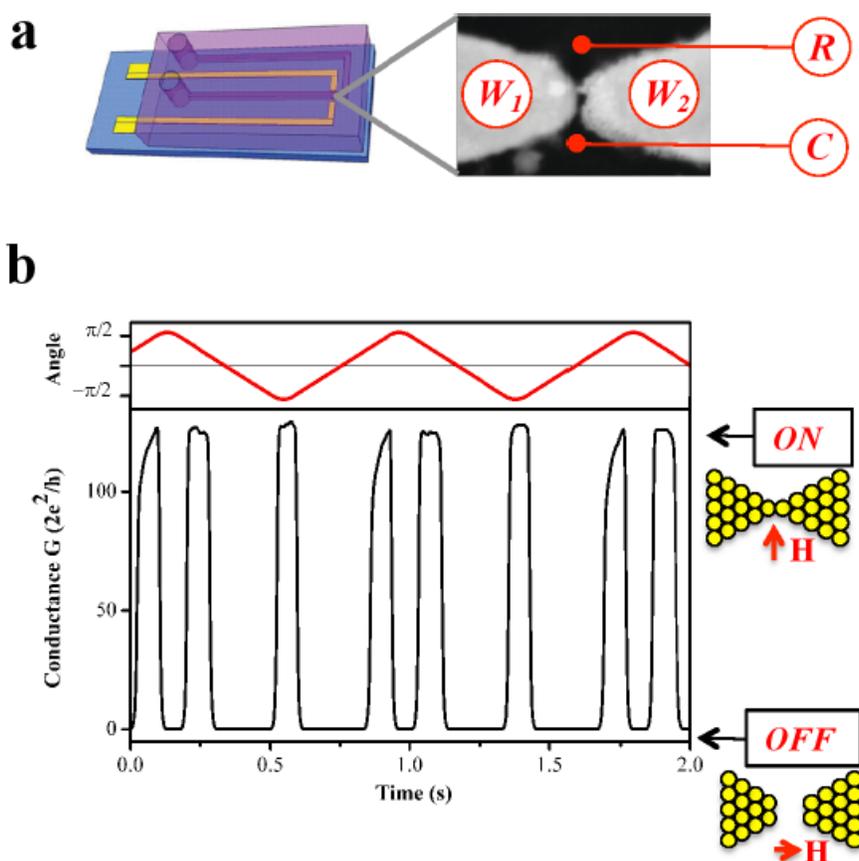
Fig. 1. Ni nanocontact construction, with ON/OFF switching of its conductance when varying the direction of the external magnetic field. a) sketch of the microfluidic cell, with electron microscopy zoom of the nano-electrodes used as working electrodes , in an

electrochemical cell including a reference *R* and a counter *C* electrodes; b) time evolution of the conductance under oscillating (0.5 Hz) rotation of the applied magnetic field of constant 0.8 Tesla amplitude. The top line represents the time oscillation of the magnetic field orientation, with an opening of the contact when the field is along the direction of the electrodes (zero angle) and closure at angles in the vicinity of ± π/2. The diagrams on the left present schematics of the related open (*OFF*) and closed (*ON*) nanocontacts.
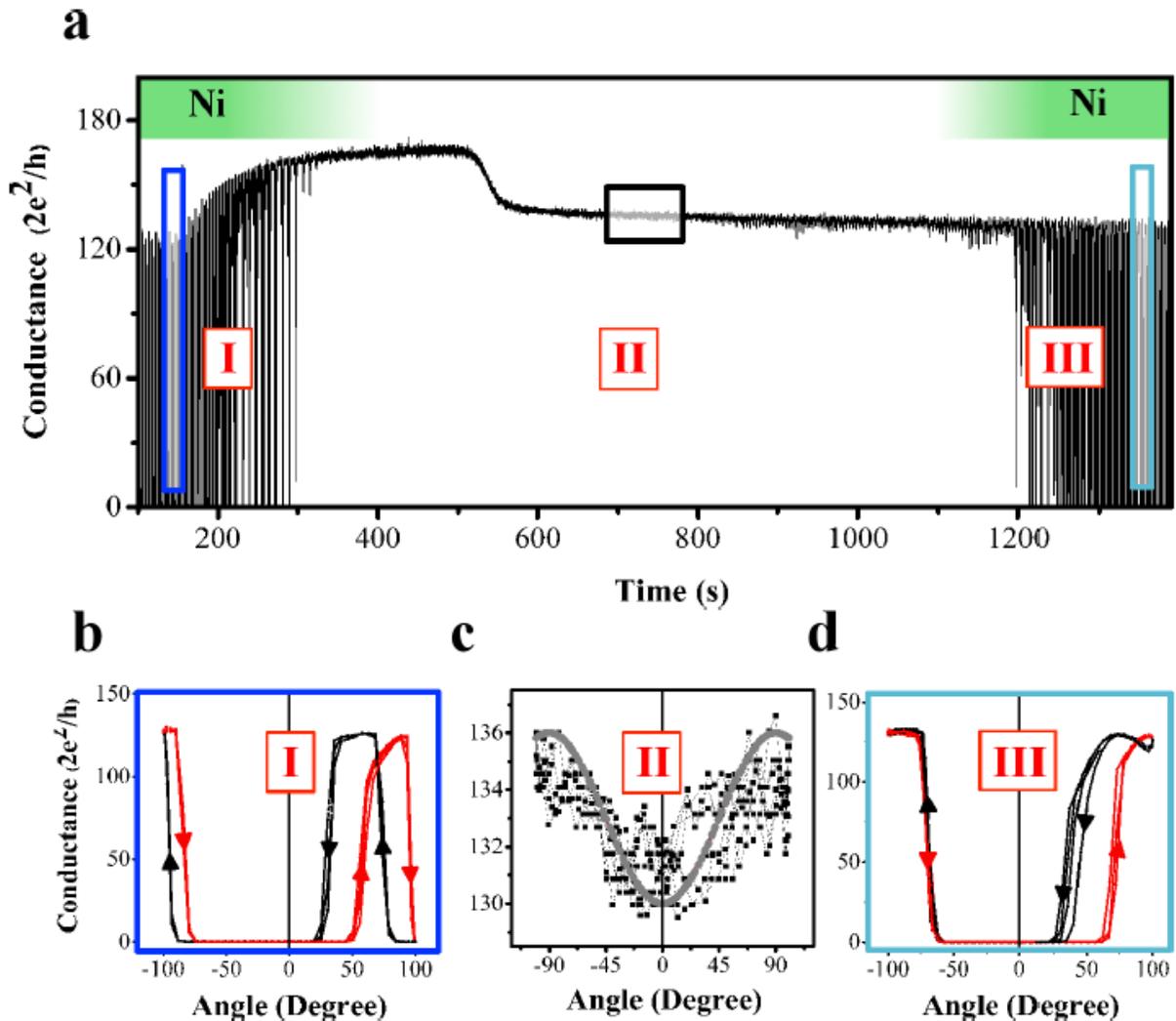
Fig. 2. Evolution of the anisotropic magnetoresistance of a Ni nanocontact when modifying the chemical environment. a) time evolution of the conductance under oscillating (0.5 Hz)

rotation of the applied magnetic field of constant 0.8 Tesla amplitude. The electroplating Ni solution is initially present (zone I), replaced with the buffer electrolyte solution (zone II) and reinstated (zone III), with the green bars indicating the presence of Ni^{++} ions. The rectangles correspond to the area used for reconstructing the AMR curves b) - d), corresponding to stages of experiments I, II, and III respectively. A fit of d), expected for a metallic bulk Ni contact, is shown. Note the color-coding in b) and d) to differentiate the sweep directions.
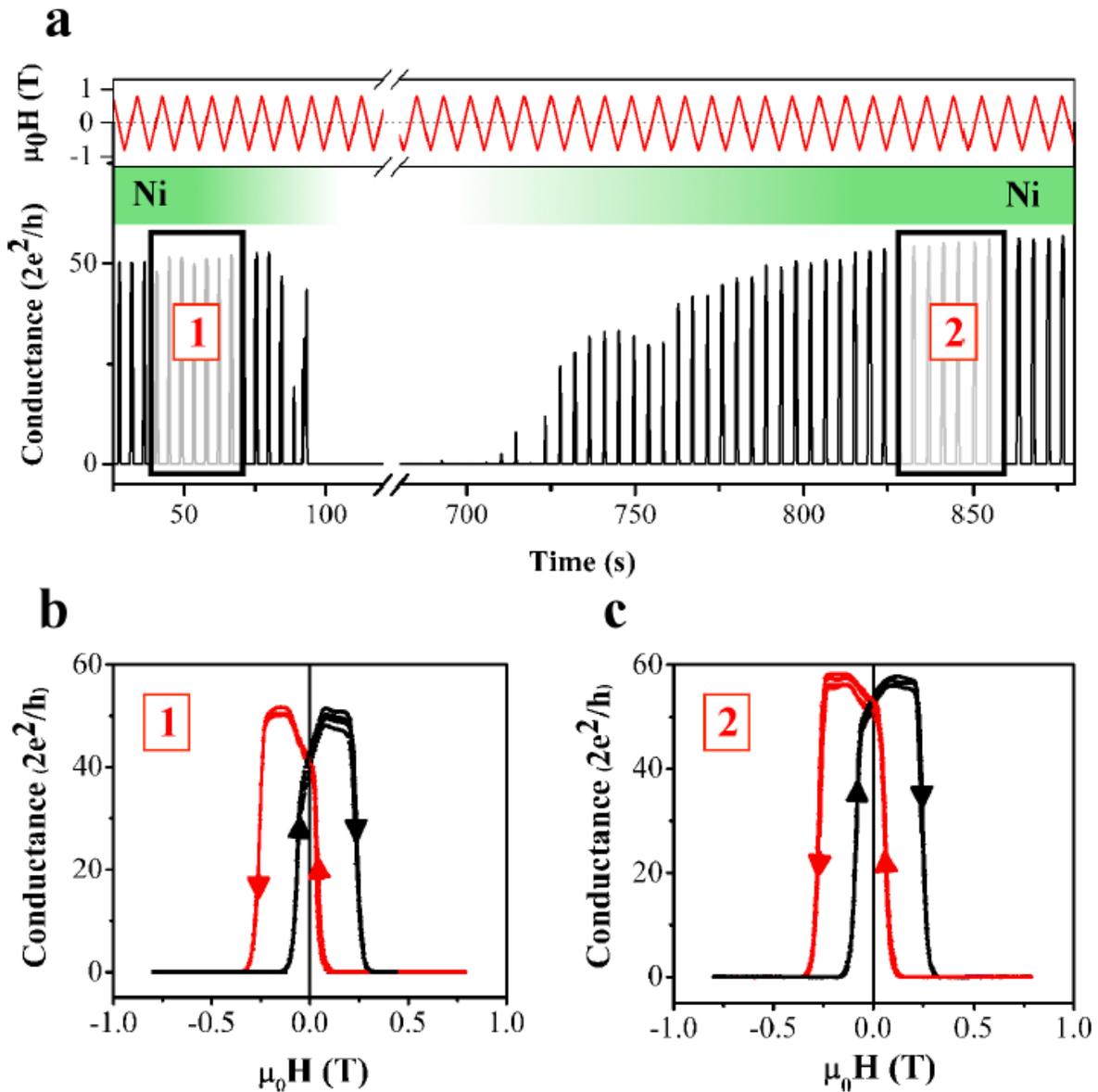
Fig. 3. Evolution of the magnetoresistance of a Ni nanocontact when modifying the chemical environment. a) time evolution of conductance during the whole experiment, with top inset showing the oscillation of the varying applied field (at two slightly different rates) between ± 0.8 T. When Ni ions are present (green area), during the initial 1 and final 2 conditions, a large oscillation of the sample conductance relates to the sweeping of the applied field. Eliminating the Ni ions from the solution results in an open contact; b) and c) related MR curves corresponding to time zones 1 and 2, indicating huge MR properties, recovered when reinstating the initial electrochemical environment.
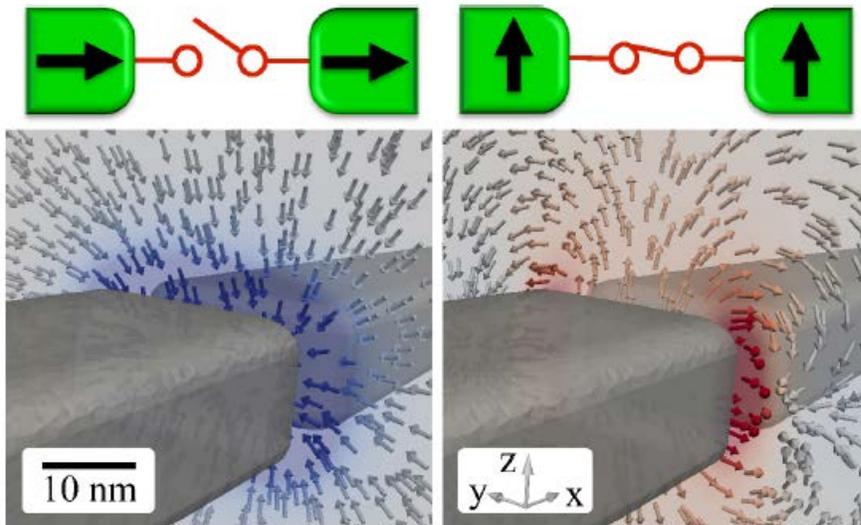
Fig. 4. Magnetic gradient force density field for nanoscale Ni electrodes. The top diagrams sketch the relaxed magnetization orientation in the electrodes, with a related broken or straight line symbolizing an open and closed electric contact. The electrodes are made of rectangular bars 300 nm long, 30 nm wide, 16 nm high, with slightly rounded corners. Left: the external field of 0.8 T magnitude is applied along the longitudinal direction x; Right: the field is applied along the transversal direction y. The vector field reveals the direction of the forces. The color code indicates the amplitude of the forces, attractive (blue) in the longitudinal case and repulsive (red) in the transverse case. The maximum color intensity corresponds to a magnitude of N/. More quantitative details can be found in the SI.